Organization of Higher-Order Oligomers of the Serotonin$_{1A}$ Receptor Explored Utilizing Homo-FRET in Live Cells

Sourav Ganguly,[†] Andrew H. A. Clayton,[‡*] and Amitabha Chattopadhyay[†*]
[†]Centre for Cellular and Molecular Biology, Council of Scientific and Industrial Research, Hyderabad, India; and [‡]Centre for Microphotonics, Faculty of Engineering and Industrial Sciences, Swinburne University of Technology, Hawthorn, Australia

ABSTRACT The serotonin$_{1A}$ receptor is a representative member of the GPCR superfamily and serves as an important drug target. The possible role of GPCR oligomerization in receptor function is an active area of research. We monitored the oligomerization state of serotonin$_{1A}$ receptors using homo-FRET and fluorescence lifetime measurements. Homo-FRET is estimated by a reduction in fluorescence anisotropy and provides a superior approach for exploring oligomerization. In addition, homo-FRET offers the possibility of detecting higher-order oligomers. On the basis of an observed increase in fluorescence anisotropy upon progressive photobleaching and analysis of the difference between the extrapolated anisotropy and the predicted anisotropy of an immobile monomer, we propose the presence of constitutive oligomers of the serotonin$_{1A}$ receptor. To the best of our knowledge, these results constitute the first report of higher-order oligomers for the serotonin$_{1A}$ receptor. We further show that cholesterol depletion and antagonist treatment result in a reduced population of higher-order oligomers. In contrast, agonist stimulation and destabilization of the actin cytoskeleton lead to an increased contribution from higher oligomers. These results provide novel insight into the oligomerization status of the serotonin$_{1A}$ receptor that could enhance the ability to design better therapeutic strategies to combat diseases related to malfunctioning of GPCRs.

INTRODUCTION

The GPCR superfamily is the largest and most diverse protein family in mammals, involved in signal transduction across membranes (1). Cellular signaling by GPCRs requires their activation by ligands present in the extracellular environment and the subsequent transduction of signals to the interior of the cell through concerted changes in their transmembrane domain structure. GPCRs mediate multiple physiological processes, including neurotransmission, cellular metabolism, secretion, cellular differentiation, growth, and inflammatory and immune responses. It is therefore only natural that GPCRs have emerged as major targets for the development of novel drug candidates in all clinical areas, and account for ~50% of current drug targets (2). The serotonin$_{1A}$ (5-HT$_{1A}$) receptor is an important member of the GPCR superfamily and is the most extensively studied among the serotonin receptors, for a variety of reasons (3). The serotonin$_{1A}$ receptor agonists and antagonists have been shown to have potential therapeutic effects in anxiety or stress-related disorders (3). As a result, the serotonin$_{1A}$ receptor serves as an important target in the development of therapeutic agents for neuropsychiatric disorders such as anxiety and depression.

Aggregation and oligomerization have often been challenging yet exciting aspects in the study of membrane proteins. An emerging area is the possible role of oligomerization in GPCR organization and signaling (4–8). The potential implications of such oligomerization are far-reaching, especially considering the role of GPCRs as major drug targets (9). Fluorescence-based resonance energy transfer methods such as hetero-FRET and bioluminescence resonance energy transfer have been used to study GPCR oligomerization in live cell membranes (8). However, these techniques are often associated with a number of inherent complications arising from the use of receptors conjugated to two different probes, and a lack of control in their relative expression levels (10,11). Hetero-FRET measurements are performed utilizing using two different fluorophores with sufficient spectral overlap. In the case of heterologously expressed proteins, the expression levels of the tagged proteins may vary, making intensity-based hetero-FRET measurements difficult to interpret. These factors have limited the usefulness of these approaches for providing information about GPCR biology. In comparison with hetero-FRET, homo-FRET represents a superior approach. Homo-FRET is a simpler variant of energy transfer because it takes place between like fluorophores and therefore requires only a single type of fluorophore. Homo-FRET (FRET between two identical fluorophores) depends on the inverse sixth power of separation between interacting fluorophores on the nanometer scale and thus is sensitive to protein oligomerization. The excitation and emission spectra of fluorophores exhibiting homo-FRET should have considerable

Submitted September 10, 2010, and accepted for publication December 8, 2010.

*Correspondence: aclayton@groupwise.swin.edu.au or amit@ccmb.res.in

Abbreviations used: 5-HT, 5-hydroxytryptamine (serotonin); 5-HT$_{1A}$R-EYFP, 5-hydroxytryptamine$_{1A}$ receptor tagged to enhanced yellow fluorescent protein; CD, cytochalasin D; DMSO, dimethyl sulphoxide; EGF, epidermal growth factor; FLIM, fluorescence lifetime imaging microscopy; FRET, fluorescence resonance energy transfer; GPCR, G-protein coupled receptor; MβCD, methyl-β-cyclodextrin; *p*-MPPI, 4-(2′-methoxy)-phenyl-1-[2′-(*N*-2″-pyridinyl)-*p*-iodobenzamido]ethyl-piperazine.

Editor: George Barisas.

0006-3495/11/01/0361/8 $2.00

doi: 10.1016/j.bpj.2010.12.3692

overlap. In other words, fluorophores with a relatively small Stokes shift will have a greater probability of undergoing homo-FRET. In addition, homo-FRET is manifested by a reduction in fluorescence anisotropy, a parameter that is largely independent of the concentration of fluorophores (12). Another serious limitation of hetero-FRET measurements is the lack of ability to distinguish dimers from higher-order oligomers. This is often crucial, particularly in a microheterogeneous environment such as the membrane, where multiple types of oligomeric clusters can coexist. Fortunately, homo-FRET measurements can provide an estimate of higher-order oligomerization (13,14).

In this work, we explored the oligomerization state of the serotonin$_{1A}$ receptor by performing homo-FRET and fluorescence lifetime measurements on CHO cells stably expressing the EYFP-tagged serotonin$_{1A}$ receptor (5-HT$_{1A}$R-EYFP). Spatial resolution was achieved by using a microscope-based approach and homo-FRET was monitored by the increase in fluorescence anisotropy upon progressive photobleaching of the receptor. In anisotropy enhancement after photobleaching measurements, fluorescence depolarization due to energy transfer is prevented by photobleaching of FRET acceptors (15). We show here that analysis of the progressive enhancement in anisotropy due to increasing photobleaching provides evidence for the existence of constitutive serotonin$_{1A}$ receptor oligomers. We further report the effects of ligands, cholesterol depletion, and cytoskeletal disruption on receptor oligomerization.

MATERIALS AND METHODS

Materials

$MgCl_2$, *p*-MPPI, $CaCl_2$, penicillin, streptomycin, gentamicin sulfate, serotonin, MβCD, and CD were obtained from Sigma (St. Louis, MO). Dulbecco's modified Eagle's medium (DMEM)/F-12 (nutrient mixture F-12, Ham; 1:1)), fetal calf serum, and geneticin (G 418) were obtained from Invitrogen Life Technologies (Carlsbad, CA). All other chemicals used were of the highest available purity. Water was purified through a Millipore (Bedford, MA) Milli-Q system and used throughout.

Cells and cell culture

CHO-K1 cells stably expressing the serotonin$_{1A}$ receptor tagged to EYFP (referred to as CHO-5-HT$_{1A}$R-EYFP) were used (~10^5 receptors/cell). Cells were grown on Lab-Tek (Nunc, Denmark) chambers in DMEM/F-12 (1:1) supplemented with 2.4 g/L of sodium bicarbonate, 10% fetal calf serum, 60 μg/mL penicillin, 50 μg/mL streptomycin, 50 μg/mL gentamicin sulfate in a humidified atmosphere with 5% CO_2 at 37°C. CHO-5-HT$_{1A}$R-EYFP cells were maintained in the above-mentioned conditions along with 300 μg/mL geneticin.

Treatment of cells

A stock solution of 2 mM CD was made in DMSO, and further concentrations were prepared upon dilution of the stock in buffer A (phosphate-buffered saline containing 1 mM $CaCl_2$ and 0.5 mM $MgCl_2$). The amount of DMSO was always <0.5% (v/v). Treatment of control cells with similar amounts of DMSO did not show any change in cellular morphology or receptor distribution. MβCD was directly dissolved in buffer A to make the desired concentration. Cells were treated with 5 μM CD and 10 mM MβCD unless otherwise mentioned. For treatment with ligands, 10 μM serotonin or *p*-MPPI was used. All experiments were performed at room temperature (~23°C).

FLIM experiments

FLIM measurements were carried out using a fluorescence lifetime imaging attachment (LIFA; Lambert Instruments, Leutingwolde, The Netherlands) mounted on an inverted microscope (TE2000U; Nikon, Japan). The tagged receptor in living cells were excited using epi-illumination with a sinusoidally modulated 470 nm LED at 40 MHz and observed with a 100x (NA 1.25) oil objective (Nikon Plan-Fluor; Nikon, Japan) through a filter set (Nikon FITC, DM505, EM 515–555 nm). The phase and modulation lifetimes were determined from a series of images taken at 12 phase settings using software provided by the manufacturer. A pseudo random recording order provided by the software was used to correct for any photobleaching (16). Rhodamine 6G in distilled water (lifetime 4.1 ns) was used as a reference (17). The mean and standard deviations for the phase and modulation lifetimes reported are from ~20 cells. We averaged the FLIM data on a cell-to-cell basis because we are interested in the statistics of a cell population.

Fluorescence anisotropy imaging microscopy

Anisotropy imaging was performed using the same setup as described for the FLIM experiments with the inclusion of a polarizer in the excitation path of the microscope and a dual-view polarizing beam splitter in the emission path before the LIFA intensifier-CCD camera. CHO-5-HT$_{1A}$R-EYFP cells were excited using epi-illumination with a 470 nm LED at constant illumination (unmodulated) and observed with a 100x (NA 1.25) oil objective, using a Nikon FITC filter, as described above. The parallel and perpendicular components of the emission were imaged synchronously on both halves of the CCD chip. Images were recorded at constant illumination as a function of time with the software provided by the manufacturer. The images were corrected for instrumental differences in the detection of parallel and perpendicular components of the emission by using Rhodamine 6G in distilled water as a reference and an anisotropy of 0.012, measured in a Varian Eclipse spectrofluorometer, as described previously (18). To correct for the depolarization caused by the high aperture objective used in this study, Rhodamine 6G was taken in solutions of varying glycerol content and anisotropies were simultaneously measured under the microscope and a Varian Eclipse spectrofluorometer. The calibration plot of the measured anisotropy of the same Rhodamine 6G solution under the microscope versus the spectrofluorometer is shown in the inset of Fig. 1. Correction for aperture depolarization in the microscope was made by multiplying the anisotropy determined under the microscope by a constant factor of 1.47, derived from the slope.

Individual cells were selected using region-of-interest tools in ImageJ (National Institutes of Health, Bethesda, MD), and the parallel ($I_{par}(t)$) and perpendicular ($I_{perp}(t)$) intensity values were analyzed as a function of illumination time. The total fluorescence as a function of time was given by

$$I(t) = I_{par}(t) + 2GI_{perp}(t),$$

where G is the correction factor for instrumental differences in detection in the parallel and perpendicular halves of the CCD. The mean anisotropy is given by

$$r(t) = \left[I_{par}(t) - GI_{perp}(t)\right]/I(t),$$

The fractional fluorescence remaining (after time zero) was calculated as

$$f(t) = [I_{t=0} - I_t]/I_{t=0}.$$

Plots of $r(t)$ versus $f(t)$ were constructed and interpreted using the theoretical framework of Yeow and Clayton (14) (see the Supporting

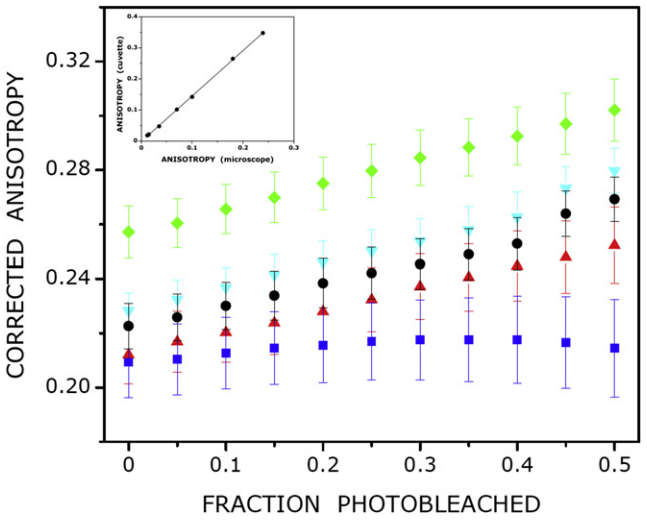

FIGURE 1 Enhancement of fluorescence anisotropy upon photobleaching of 5-HT_{1A}R-EYFP in live CHO cells under various conditions. Plots of corrected anisotropy for untreated cells (●, *black*) and cells treated with serotonin (▲, *red*), *p*-MPPI (▼, *cyan*), CD (■, *blue*), or MβCD (◆, *green*) upon photobleaching are shown. The fraction of photobleached fluorophores was binned (bin width 0.05) and the mean anisotropy and associated standard error for each bin are plotted. The inset shows the calibration plot for correction of measured anisotropy. The anisotropy values of Rhodamine 6G in solutions of increasing glycerol concentration measured in a spectrofluorometer are plotted against the anisotropy values of the same samples measured under a microscope. The calibration plot shows an excellent linear correlation ($y = 1.4699x - 0.0019$; $R^2 = 0.99$). See Materials and Methods for other details.

Material). The fraction of photobleached fluorophores was binned (bin width 0.05), and the mean anisotropy and associated standard error for each bin are plotted in Fig. 1. The mean and standard deviations reported here are from seven to eight cells for each condition, acquired over multiple sets of measurements. Image arithmetic was performed in ImageJ (National Institutes of Health). Plotting and analysis were carried out with the use of Origin software version 7.0 (OriginLab, Northampton, MA) and Microsoft (Redmond, WA) Excel 2007.

RESULTS

Fluorescence anisotropy of 5-HT_{1A}R-EYFP in live cells

We have earlier characterized the heterologously expressed serotonin$_{1A}$ receptor tagged to EYFP in CHO cells and showed that the tagged receptors are essentially similar to the native receptor (19). To explore fluorophore-fluorophore interactions due to possible oligomerization, we compared the previously reported anisotropy of EYFP in solution with that of 5-HT_{1A}R-EYFP in cells. In a dilute solution, the steady-state anisotropy would reflect the rotational motion of the monomeric fluorophore. If the fluorophore undergoes homo-FRET (for example, due to oligomerization), the emission will be depolarized, resulting in a reduced steady-state anisotropy. Homo-FRET reduces steady-state anisotropy because energy transfer from an initially excited fluorophore to one in a different orientation alters the angular distribution of emitting fluorophores from that produced by photoselection alone. In other words, homo-FRET leads to depolarization of the emission because of the lack of correlation between the orientation of the secondarily excited molecules and that of the initially photoselected donor (20). Therefore, the formation of oligomers that bring individual 5-HT_{1A}R-EYFP molecules within the homo-FRET range (~6 nm (21)) can be determined by measurement of the steady-state anisotropy.

For fluorophore-fluorophore interactions caused by oligomerization of the 5-HT_{1A}R-EYFP in the cellular plasma membrane, rapid anisotropy decay and a correspondingly lower steady-state anisotropy is predicted. Since the fundamental anisotropy (r_o) of EYFP is 0.38 (22), we assumed the fundamental anisotropy (r_o) of 5-HT_{1A}R-EYFP to be ~0.38. Our assumption is based on previous studies in which it was observed that GFP, when fused at the end of proteins, reports on segmental rather than whole protein rotational motion (23,24). Although the steady-state anisotropy of 5-HT_{1A}R-EYFP is expected to be lower than 0.38 (for example, the steady-state anisotropy of YFP in solution has been reported to be ~0.3 (25)), the orientation of the receptor in the plasma membrane may increase the anisotropy. Therefore, we used a value for the anisotropy in the absence of homo-FRET, i.e., the value for rotationally immobile EYFP (0.38). This is a reasonable approximation because reported anisotropies of GFP molecules attached to membrane proteins in the absence of homo-FRET tend to approach this value (0.36 for GFP-tagged EGF receptor (20)). Importantly, the value of 0.38 is consistent with the value used for monomeric anisotropy of GFP-tagged (via flexible linkers) to proteins (26). In any event, it should be emphasized that the fundamental anisotropy of 5-HT_{1A}R-EYFP (hereafter referred to as the predicted anisotropy of the monomer) assumed by us in this work merely serves as a reference to quantitatively monitor changes in the oligomeric state of the receptor.

All anisotropies reported here were corrected for microscopic aperture-induced depolarization (27,28) (see Materials and Methods, and *inset* in Fig. 1). We observed a significantly low initial anisotropy of ~0.22 for 5-HT_{1A}R-EYFP in control cells (see Table 1 and Fig. 1). Since the rotational correlation time of EYFP in solution is ~16 ns (22), and the fluorescence lifetime of 5-HT_{1A}R-EYFP is

TABLE 1 Anisotropy enhancement upon photobleaching of 5-HT_{1A}R-EYFP in live cells

	Anisotropy	
Condition	Initial (± SD)	Extrapolated
Control	0.223 ± 0.024	0.313
Serotonin	0.212 ± 0.026	0.293
p-MPPI	0.228 ± 0.016	0.326
CD	0.209 ± 0.034	0.225
MβCD	0.257 ± 0.023	0.347

See Materials and Methods for other details.

~3.5 ns (see below), it is unlikely that the depolarization of emission is influenced by the rotational mobility of the fluorophore. We therefore attribute the depolarization of emission to energy transfer (homo-FRET) between oligomers of 5-HT_{1A}R-EYFP molecules.

If the reduction in anisotropy is due to homo-FRET induced by oligomerization, the anisotropy should increase upon photodestruction of energy transfer acceptors (15). Fig. 1 shows the plot of the average steady-state anisotropy as a function of the extent of photobleaching of 5-HT_{1A}R-EYFP in CHO cells. An increase in fluorescence anisotropy is observed, as expected for a system undergoing homo-FRET. Assuming photobleaching to be random, the nature of this plot can be deduced for various types of oligomers from the theoretical formalism previously proposed by Yeow and Clayton (14). Fig. 2 shows the predicted variation of fluorescence anisotropy with increased photobleaching for a homogeneous distribution of monomers, dimers, trimers, and tetramers (assuming an anisotropy of 0.38 for monomers; see the Supporting Material for details). In principle, the oligomeric state and inherent mobility of the 5-HT_{1A}R-EYFP complex can be obtained by fitting the anisotropy bleaching data to the theoretical model. In that case, the extrapolated anisotropy of 5-HT_{1A}R-EYFP at the 100% photobleaching limit should reflect the inherent rotational mobility of 5-HT_{1A}R-EYFP (i.e., in the absence of homo-FRET). However, it is difficult to achieve a very high degree of fractional bleaching experimentally because of possible cytotoxic effects and reduction in the signal/noise ratio. To avoid these problems associated with high fractional bleaching, we compared the linearly extrapolated anisotropy with the predicted anisotropy to infer the presence of higher-order oligomers (shown in Fig. 2). The closer the extrapolated anisotropy is to the predicted anisotropy (0.38), the higher is the fraction of dimeric population. On the other hand, the larger the difference between the extrapolated and predicted anisotropy, the greater is the fraction of higher-order ($N > 2$) oligomers. A comparison of Figs. 1 and 2 shows that although data for the serotonin$_{1A}$ receptor under control conditions could be well fitted by a linear model, the extrapolated and predicted anisotropies exhibit a considerable difference (Table 1). Interestingly, the extrapolated anisotropy in control cells was found to be ~0.31 (see Table 1). We therefore interpret the lower value of the extrapolated anisotropy to be due to the presence of higher-order ($N > 2$) oligomers of 5-HT_{1A}R-EYFP (see Fig. 2).

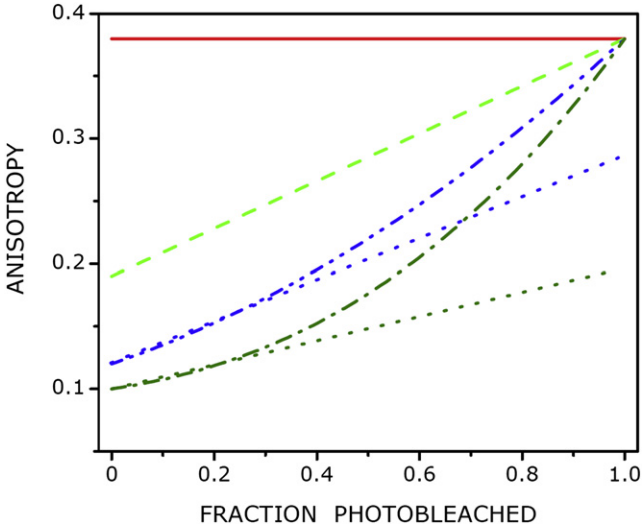

FIGURE 2 Simulation of anisotropy enhancement upon photobleaching for a population of homogeneous oligomers containing N subunits. N-values correspond to 1 (monomer, *red* —), 2 (dimer, *light green* —-), 3 (trimer, *blue* — - - —), and 4 (tetramer, *deep green* — - —). Simulations were generated using the theoretical formalism developed by Yeow and Clayton (14). The extrapolated anisotropies derived from initial points corresponding to fractional bleaching (<0.3) in the case of trimer and tetramer are also shown (……). See Materials and Methods for other details.

Effect of ligand stimulation on receptor oligomerization

To monitor the effect of ligand stimulation on oligomerization of 5-HT_{1A}R-EYFP, we measured the increase in fluorescence anisotropy subsequent to photobleaching upon treatment with agonist (serotonin) and antagonist (*p*-MPPI). As shown in Fig. 1 and Table 1, the increase in anisotropy upon photobleaching in both cases was linear, as observed in the case of control cells. A comparison with the extrapolated anisotropy in the case of ligand stimulation brings up an interesting point (see Table 1 and Fig. 3). While the extrapolated anisotropy increases (i.e., approaches the

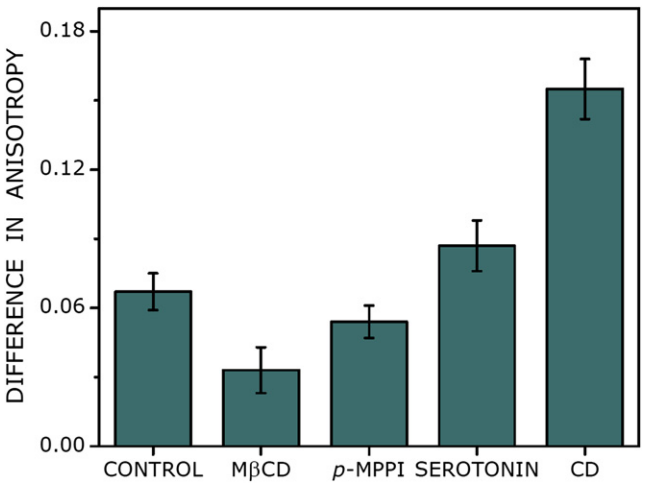

FIGURE 3 Difference between the extrapolated anisotropy (extrapolated to complete photobleaching) and the predicted anisotropy of 5-HT_{1A}R-EYFP plotted under various conditions. The extrapolated anisotropy is estimated from a linear fit of the photobleaching data (see Fig. 1 and Table 1). With increasing oligomerization, the extrapolated anisotropy is expected to increasingly deviate from the predicted anisotropy. The magnitude of deviation provides a measure of the extent of oligomerization. See text for other details.

predicted anisotropy (~0.38)) in case of stimulation by the antagonist (compared with the extrapolated anisotropy observed for control cells), the extrapolated anisotropy upon agonist stimulation is lower. These results suggest that although antagonist treatment results in lowering the fraction of higher-order oligomers compared with what is present in control conditions, the agonist appears to induce the formation of higher-order oligomers.

Effect of cholesterol depletion on receptor oligomerization

Cholesterol has been shown to improve the stability of various GPCRs, such as the β_2-adrenergic receptor (29), and appears to be a necessary component for crystallization of the receptor because it is believed to facilitate receptor-receptor interaction and consequent oligomerization (30). To explore the effect of membrane cholesterol on the oligomerization of 5-HT_{1A}R-EYFP, we treated cells with the cholesterol-depleting agent MβCD. As shown in Fig. 1 and Table 1, the increase in anisotropy upon photobleaching in MβCD-treated cells was linear. In the case of cholesterol-depleted cells, the initial anisotropy (~0.26) appears to be higher than in control cells (Table 1). The extrapolated anisotropy, on the other hand, approaches much closer to the predicted anisotropy (see Table 1 and Fig. 3). These results imply the predominance of a receptor dimer population in the cholesterol-depleted condition. In other words, a fraction of higher-order oligomers (present under control conditions) are reduced to dimers upon cholesterol depletion. We therefore conclude that higher-order oligomers of the receptor are more stringently regulated by membrane cholesterol than dimers.

Actin cytoskeleton destabilization leads to reorganization of the receptor oligomeric population

We have previously shown that the actin cytoskeleton regulates the mobility and signaling of the serotonin$_{1A}$ receptor (31–33). To monitor the effects of the actin cytoskeleton on receptor oligomerization, we measured the change in 5-HT_{1A}R-EYFP anisotropy after photobleaching upon destabilization of the actin cytoskeleton by CD. Interestingly, actin cytoskeleton destabilization resulted in a very different nature of the recovery of fluorescence anisotropy upon photobleaching (Fig. 1 and Table 1). As shown in the figure, the increase in anisotropy upon photobleaching of the receptor was marginal in this case, in sharp contrast to the above results. The initial anisotropy of 5-HT_{1A}R-EYFP was somewhat lower in CD-treated cells than in the control condition. The trend in increase of anisotropy upon photobleaching was very different under this condition. This becomes apparent upon comparison of the extrapolated anisotropy for actin destabilization with that obtained under other conditions (see Fig. 3 and Table 1). As shown in the figure and table, the extrapolated anisotropy was considerably lower than the predicted anisotropy, implying a significant extent of receptor clustering into higher-order oligomers. These results suggest that upon destabilization of the actin cytoskeleton, the serotonin$_{1A}$ receptor undergoes reorganization to form larger oligomers.

Fluorescence lifetime of 5-HT_{1A}R-EYFP in cells

The lifetime of a fluorophore is known to be sensitive to its immediate environment (34). An image of the fluorescence lifetime distribution of a given fluorophore in a cellular milieu can provide location-specific environmental information (35). We assessed the sensitivity of the fluorescence lifetime of 5-HT_{1A}R-EYFP under conditions described above using frequency domain FLIM of live cells. The spatial distribution of the fluorescence lifetime of 5-HT_{1A}R-EYFP, color-coded on a scale of 0–4 ns, is shown in Fig. 4. The phase and modulation lifetime images in control cells show general agreement with average lifetimes of 3.55 and 3.69 ns, respectively. The close agreement of the phase and modulation lifetimes suggests that the EYFP fluorophore experiences an overall homogeneous environment inside the cell (36). We did not observe any significant distribution in the fluorescence lifetime of 5-HT_{1A}R-EYFP in the cell (Fig. 4), which suggests that the EYFP lifetime is relatively insensitive to the cellular microenvironment in which it is localized. This is not surprising considering the fact that the fluorophore moiety of the GFP group of proteins has been shown to be insensitive to the bulk environment due to its compact β-barrel structure (37). In addition, the average fluorescence lifetime of 5-HT_{1A}R-EYFP remained invariant (see Table 2), even in conditions where we observed maximal changes in receptor oligomerization status (i.e., cholesterol depletion and actin cytoskeleton destabilization; see Table 1). Importantly, these results assume significance because the overall invariance of the measured lifetime suggests that the anisotropy measurements described above are not influenced by a change in the fluorescence lifetime.

Fluorescence anisotropy of 5-HT_{1A}R-EYFP in cells is independent of receptor expression

Oligomerization of membrane proteins can be induced by trivial association due to overexpression of a given protein. For example, it was previously reported that although neurokinin-1 receptor may appear to oligomerize at higher expression levels, it is monomeric at low levels of expression (11). To avoid such artifacts, we analyzed the dependence of the measured initial anisotropy on receptor expression levels. To that end, we measured the total fluorescence intensity originating from a cell and the corresponding anisotropy of the same cell. Data points from all

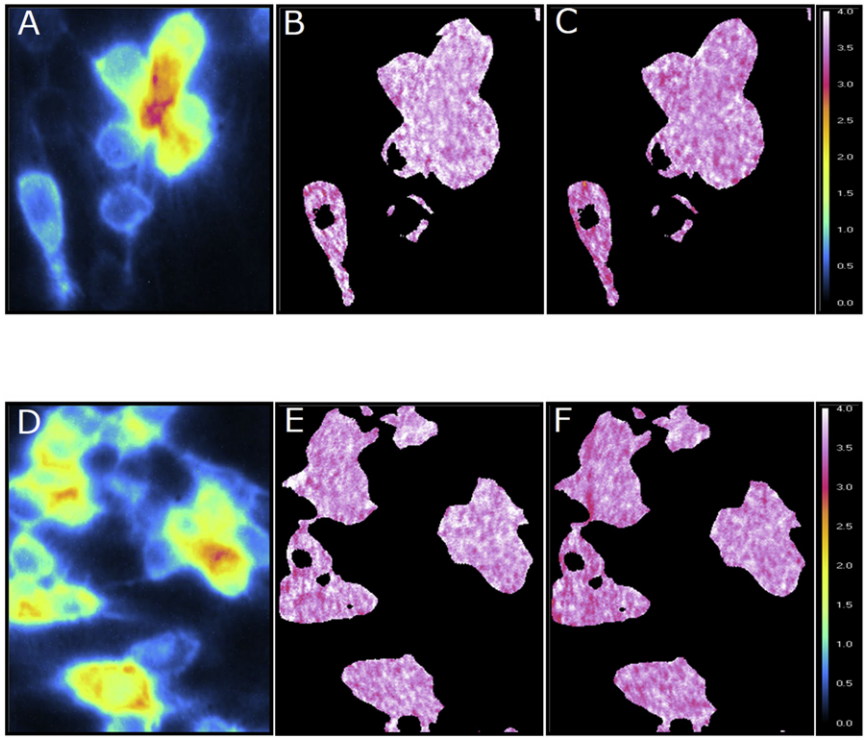

FIGURE 4 Frequency domain FLIM of CHO-5-HT_{1A}R-EYFP cells. Panels *A–C* show the intensity (*blue*: low, *white*: high), modulation, and phase lifetime images (color-coded on a scale of 0–4 ns) of untreated cells. Images represent the spatial distribution of fluorescence intensity, modulation, and phase lifetimes of 5-HT_{1A}R-EYFP. Panels *D–F* show the corresponding images of cells treated with CD. See Materials and Methods for other details.

treatments analyzed this way and the resulting scatter is shown in Fig. 5. The figure shows that our data set includes receptors that differ in expression levels by ~4-fold, since we observe a similar fold change in fluorescence intensity. Notably, the absence of any specific trend in the scatter shows that the measured anisotropies were independent of receptor expression level. We therefore conclude that the oligomeric status of the serotonin$_{1A}$ receptor reported by us is independent of the receptor expression levels.

DISCUSSION

In this work, we monitored the oligomerization state of the serotonin$_{1A}$ receptor using homo-FRET. On the basis of the observed increase in fluorescence anisotropy upon progressive photobleaching, and our analysis of data based on the difference between the extrapolated anisotropy and the predicted anisotropy, we propose the presence of constitutive oligomers of the serotonin$_{1A}$ receptor. Previous studies focused on the oligomerization state of the serotonin$_{1A}$ receptor (38–40) using either hetero-FRET (39,40) or coimmunoprecipitation (38). As noted above, hetero-FRET suffers from a number of limitations, and immunological approaches are susceptible to cross-reactivity. In our work, we utilized homo-FRET, which is free from these

TABLE 2 Comparison of phase and modulation lifetimes of 5-HT_{1A}R-EYFP in live cells

Condition	Phase lifetime τ_φ (± SD) (ns)	Modulation lifetime τ_M (± SD) (ns)
Control	3.55 ± 0.09	3.69 ± 0.05
CD	3.54 ± 0.03	3.66 ± 0.02
MβCD	3.46 ± 0.06	3.66 ± 0.04

See Materials and Methods for other details.

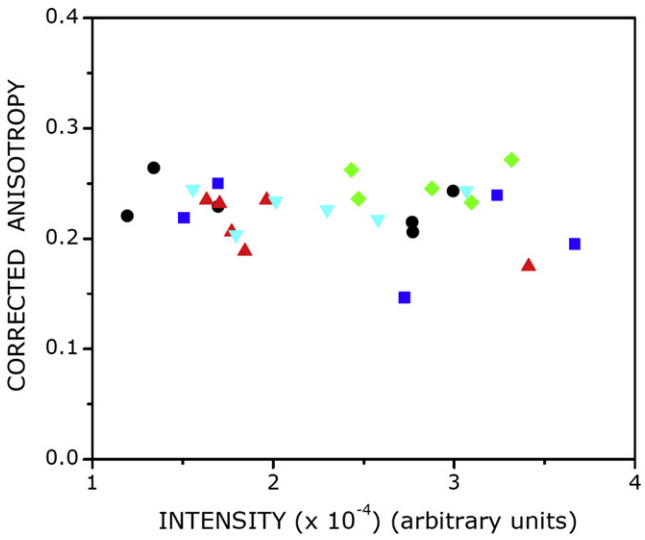

FIGURE 5 Fluorescence intensity from a large number of measurements ($N > 25$) plotted against the corresponding values of initial anisotropy. The plotted points represent data collected under conditions described in Fig. 1 (untreated cells (●, *black*) and cells treated with serotonin (▲, *red*), *p*-MPPI (▼, *cyan*), CD (■, *blue*), or MβCD (◆, *green*)). It is apparent that there is no systematic variation of anisotropy with intensity (receptor number). See Materials and Methods for other details.

limitations. A unique advantage of homo-FRET is that it allows one to detect higher-order oligomers along with dimers (14). To our knowledge, this study is the first to suggest the presence of higher-order oligomers of the serotonin$_{1A}$ receptor. Interestingly, such higher-order oligomers have recently been implicated in the case of the EGF receptor (41). In addition, we report the reorganization of higher-order oligomers in response to ligand activation, membrane cholesterol depletion, and actin cytoskeleton destabilization (see Fig. 6).

We observe that agonist (serotonin) stimulation and cytoskeletal destabilization appear to reduce the initial anisotropy, whereas antagonist (*p*-MPPI) treatment and cholesterol depletion lead to an increase in initial anisotropy. In addition, the difference between the extrapolated anisotropy and the predicted anisotropy is greater for agonist stimulation and cytoskeletal destabilization, and less for antagonist treatment and cholesterol depletion (Fig. 3). These results suggest that antagonist treatment and cholesterol depletion effectively reduce the population of higher-order oligomers. In contrast, agonist stimulation and destabilization of the actin cytoskeleton lead to an increased contribution from higher oligomers (see Fig. 6). Importantly, the increase in anisotropy upon photobleaching remains linear within experimental limits in all cases, suggesting the significant presence of dimers. In the case of actin cytoskeleton destabilization, we observe a major loss in recovery in anisotropy upon photobleaching and a severe reduction in the extrapolated anisotropy (Fig. 1). This could be interpreted as resulting from the formation of larger oligomers under this condition.

Our current understanding of the organization of biological membranes involves the concept of lateral heterogeneities in the membrane, collectively termed as membrane domains (42,43). These lateral heterogeneities are further modulated by cholesterol and actin cytoskeleton. A comprehensive understanding of cellular signaling would therefore require the mapping of membrane heterogeneity at both spatial and temporal scales under these conditions. In view of the overall spatiotemporal heterogeneity of the eukaryotic plasma membrane, it is conceivable that segregated domains of the plasma membrane can harbor different oligomeric forms of GPCRs. The total population of receptors could therefore exist in a dynamic equilibrium between such domains. In view of the enormous implications of GPCR function in human health, progress in elucidating the oligomerization status of GPCRs would enhance our ability to design better therapeutic strategies to combat diseases related to malfunctioning of these receptors.

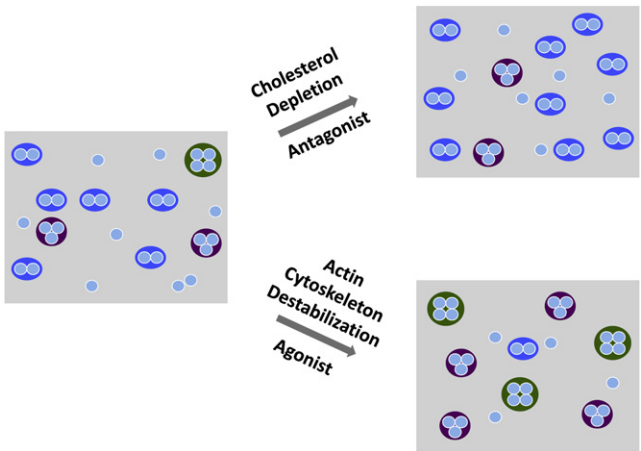

FIGURE 6 Schematic model of the oligomeric status of the serotonin$_{1A}$ receptor. The model assumes an initial state of heterogeneous oligomers of the receptor in an untreated (control) cell membrane. Upon activation with agonist or destabilization of the actin cytoskeleton, receptors tend to form oligomeric structures of higher order (>2 monomers/cluster). Antagonist treatment or cholesterol depletion appears to increase the fraction of receptor population in the dimeric state. See text for other details.

SUPPORTING MATERIAL

Additional text and references are available at http://www.biophysj.org/biophysj/supplemental/S0006-3495(10)05207-0.

We thank members of A.C.'s research group for critically reading the manuscript.

This work was supported by a Fluorescence Applications in Biotechnology and Life Sciences grant from the Australian Research Council and the National Health and Medical Research Council, Australia (to A.C. and A.H.A.C.). In addition, work in A.C.'s laboratory was supported by the Council of Scientific and Industrial Research, India. A.H.A.C. acknowledges support from R.D. Wright Biomedical Career Development Award from the National Health and Medical Research Council. S.G. thanks the Council of Scientific and Industrial Research for the award of a Senior Research Fellowship. A.C. is an Adjunct Professor at the Special Centre for Molecular Medicine of Jawaharlal Nehru University (New Delhi, India) and the Indian Institute of Science Education and Research (Mohali, India), and Honorary Professor of the Jawaharlal Nehru Centre for Advanced Scientific Research (Bangalore, India). A.C. gratefully acknowledges J.C. Bose Fellowship (Department of Science and Technology, India).

REFERENCES

1. Rosenbaum, D. M., S. G. F. Rasmussen, and B. K. Kobilka. 2009. The structure and function of G-protein-coupled receptors. *Nature.* 459:356–363.
2. Heilker, R., M. Wolff, …, M. Bieler. 2009. G-protein-coupled receptor-focused drug discovery using a target class platform approach. *Drug Discov. Today.* 14:231–240.
3. Pucadyil, T. J., S. Kalipatnapu, and A. Chattopadhyay. 2005. The serotonin$_{1A}$ receptor: a representative member of the serotonin receptor family. *Cell. Mol. Neurobiol.* 25:553–580.
4. Shanti, K., and A. Chattopadhyay. 2000. A new paradigm in the functioning of G-protein-coupled receptors. *Curr. Sci.* 79:402–403.
5. Angers, S., A. Salahpour, and M. Bouvier. 2002. Dimerization: an emerging concept for G protein-coupled receptor ontogeny and function. *Annu. Rev. Pharmacol. Toxicol.* 42:409–435.
6. Park, P. S., S. Filipek, …, K. Palczewski. 2004. Oligomerization of G protein-coupled receptors: past, present, and future. *Biochemistry.* 43:15643–15656.
7. Milligan, G. 2007. G protein-coupled receptor dimerisation: molecular basis and relevance to function. *Biochim. Biophys. Acta.* 1768:825–835.

8. Lohse, M. J. 2010. Dimerization in GPCR mobility and signaling. *Curr. Opin. Pharmacol.* 10:53–58.
9. George, S. R., B. F. O'Dowd, and S. P. Lee. 2002. G-protein-coupled receptor oligomerization and its potential for drug discovery. *Nat. Rev. Drug Discov.* 1:808–820.
10. James, J. R., M. I. Oliveira, …, S. J. Davis. 2006. A rigorous experimental framework for detecting protein oligomerization using bioluminescence resonance energy transfer. *Nat. Methods.* 3:1001–1006.
11. Meyer, B. H., J.-M. Segura, …, H. Vogel. 2006. FRET imaging reveals that functional neurokinin-1 receptors are monomeric and reside in membrane microdomains of live cells. *Proc. Natl. Acad. Sci. USA.* 103:2138–2143.
12. Tramier, M., T. Piolot, …, M. Coppey-Moisan. 2003. Homo-FRET versus hetero-FRET to probe homodimers in living cells. *Methods Enzymol.* 360:580–597.
13. Runnels, L. W., and S. F. Scarlata. 1995. Theory and application of fluorescence homotransfer to melittin oligomerization. *Biophys. J.* 69:1569–1583.
14. Yeow, E. K. L., and A. H. A. Clayton. 2007. Enumeration of oligomerization states of membrane proteins in living cells by homo-FRET spectroscopy and microscopy: theory and application. *Biophys. J.* 92:3098–3104.
15. Varma, R., and S. Mayor. 1998. GPI-anchored proteins are organized in submicron domains at the cell surface. *Nature.* 394:798–801.
16. van Munster, E. B., and T. W. J. Gadella, Jr. 2004. Suppression of photobleaching-induced artifacts in frequency-domain FLIM by permutation of the recording order. *Cytometry A.* 58:185–194.
17. Magde, D., G. E. Rojas, and P. G. Seybold. 1999. Solvent dependence of the fluorescence lifetimes of xanthene dyes. *Photochem. Photobiol.* 70:737–744.
18. Clayton, A. H. A., Q. S. Hanley, …, T. M. Jovin. 2002. Dynamic fluorescence anisotropy imaging microscopy in the frequency domain (rFLIM). *Biophys. J.* 83:1631–1649.
19. Pucadyil, T. J., S. Kalipatnapu, …, A. Chattopadhyay. 2004. G-protein-dependent cell surface dynamics of the human serotonin$_{1A}$ receptor tagged to yellow fluorescent protein. *Biochemistry.* 43:15852–15862.
20. Lidke, D. S., P. Nagy, …, T. M. Jovin. 2003. Imaging molecular interactions in cells by dynamic and static fluorescence anisotropy (rFLIM and emFRET). *Biochem. Soc. Trans.* 31:1020–1027.
21. Patterson, G. H., D. W. Piston, and B. G. Barisas. 2000. Förster distances between green fluorescent protein pairs. *Anal. Biochem.* 284:438–440.
22. Borst, J. W., M. A. Hink, …, A. J. Visser. 2005. Effects of refractive index and viscosity on fluorescence and anisotropy decays of enhanced cyan and yellow fluorescent proteins. *J. Fluoresc.* 15:153–160.
23. Rocheleau, J. V., M. Edidin, and D. W. Piston. 2003. Intrasequence GFP in class I MHC molecules, a rigid probe for fluorescence anisotropy measurements of the membrane environment. *Biophys. J.* 84: 4078–4086.
24. Hink, M. A., R. A. Griep, …, A. J. Visser. 2000. Structural dynamics of green fluorescent protein alone and fused with a single chain Fv protein. *J. Biol. Chem.* 275:17556–17560.
25. Shi, X., J. Basran, …, S. G. Boxer. 2007. Anomalous negative fluorescence anisotropy in yellow fluorescent protein (YFP 10C): quantitative analysis of FRET in YFP dimers. *Biochemistry.* 46:14403–14417.
26. Bader, A. N., E. G. Hofman, …, H. C. Gerritsen. 2009. Homo-FRET imaging enables quantification of protein cluster sizes with subcellular resolution. *Biophys. J.* 97:2613–2622.
27. Axelrod, D. 1979. Carbocyanine dye orientation in red cell membrane studied by microscopic fluorescence polarization. *Biophys. J.* 26: 557–573.
28. Piston, D. W., and M. A. Rizzo. 2008. FRET by fluorescence polarization microscopy. *Methods Cell Biol.* 85:415–430.
29. Yao, Z., and B. Kobilka. 2005. Using synthetic lipids to stabilize purified β_2 adrenoceptor in detergent micelles. *Anal. Biochem.* 343: 344–346.
30. Cherezov, V., D. M. Rosenbaum, …, R. C. Stevens. 2007. High-resolution crystal structure of an engineered human β_2-adrenergic G protein-coupled receptor. *Science.* 318:1258–1265.
31. Ganguly, S., T. J. Pucadyil, and A. Chattopadhyay. 2008. Actin cytoskeleton-dependent dynamics of the human serotonin$_{1A}$ receptor correlates with receptor signaling. *Biophys. J.* 95:451–463.
32. Ganguly, S., P. Singh, …, A. Chattopadhyay. 2009. Differential dynamics of membrane proteins in yeast. *Biochem. Biophys. Res. Commun.* 387:661–665.
33. Ganguly, S., and A. Chattopadhyay. 2010. Cholesterol depletion mimics the effect of cytoskeletal destabilization on membrane dynamics of the serotonin$_{1A}$ receptor: A zFCS study. *Biophys. J.* 99:1397–1407.
34. Prendergast, F. G. 1991. Time-resolved fluorescence techniques: methods and applications in biology. *Curr. Opin. Struct. Biol.* 1:1054–1059.
35. de Almeida, R. F., L. M. Loura, and M. Prieto. 2009. Membrane lipid domains and rafts: current applications of fluorescence lifetime spectroscopy and imaging. *Chem. Phys. Lipids.* 157:61–77.
36. Lakowicz, J. R. 2006. Principles of Fluorescence Spectroscopy, 3rd ed. Springer, New York.
37. Haldar, S., and A. Chattopadhyay. 2007. Dipolar relaxation within the protein matrix of the green fluorescent protein: a red edge excitation shift study. *J. Phys. Chem. B.* 111:14436–14439.
38. Salim, K., T. Fenton, …, P. C. Guest. 2002. Oligomerization of G-protein-coupled receptors shown by selective co-immunoprecipitation. *J. Biol. Chem.* 277:15482–15485.
39. Kobe, F., U. Renner, …, E. Ponimaskin. 2008. Stimulation- and palmitoylation-dependent changes in oligomeric conformation of serotonin 5-HT$_{1A}$ receptors. *Biochim. Biophys. Acta.* 1783:1503–1516.
40. Łukasiewicz, S., E. Błasiak, …, M. Dziedzicka-Wasylewska. 2007. Fluorescence studies of homooligomerization of adenosine A_{2A} and serotonin 5-HT$_{1A}$ receptors reveal the specificity of receptor interactions in the plasma membrane. *Pharmacol. Rep.* 59:379–392.
41. Clayton, A. H. A., S. G. Orchard, …, A. W. Burgess. 2008. Predominance of activated EGFR higher-order oligomers on the cell surface. *Growth Factors.* 26:316–324.
42. Mukherjee, S., and F. R. Maxfield. 2004. Membrane domains. *Annu. Rev. Cell Dev. Biol.* 20:839–866.
43. Jacobson, K., O. G. Mouritsen, and R. G. W. Anderson. 2007. Lipid rafts: at a crossroad between cell biology and physics. *Nat. Cell Biol.* 9:7–14.

Biophysical Journal

Organization of Higher-Order Oligomers of the Serotonin$_{1A}$ Receptor Explored by Homo-FRET in Live Cells

Sourav Ganguly, Andrew H. A. Clayton, and Amitabha Chattopadhyay

We first discuss the case of a dilute population of molecules tagged to a fluorophore in a given state of oligomerization using the theoretical framework developed earlier (1). We assume that all the molecules are fluorescently tagged and their fluorescence properties are uniform. Each oligomeric species is characterized by its anisotropy, *i.e.*, an oligomeric species with i monomers will exhibit an anisotropy of r_i (*e.g.*, r_1, r_2, r_3 and r_4 will be the anisotropy for pure monomer, dimer, trimer and tetramer, respectively).

The anisotropy of the monomer (r_1) is greater than the higher (N > 1) oligomeric forms due to depolarization of fluorescence emission by homo-FRET in case of oligomers. This gives rise to the condition:

$$r_1 > r_2 > r_3 > r_4$$

The anisotropy for an N-mer (an oligomer with N monomers) can be assumed to be r_1/N. Strictly speaking, this choice of anisotropy corresponds to the limit of efficient energy migration between randomly oriented yet rotationally fixed fluorophores. Although this condition may not be valid in the present case, r_i would still be a function of i.

The effect of photobleaching on the fluorescence anisotropy of such a population of homogeneous oligomers can be described as discussed below. For the case of a monomeric population, homo-FRET would be absent (by definition). Photobleaching of such a population therefore will not lead to any change in anisotropy. For a monomeric population, the anisotropy would be independent of the fractional photobleaching (denoted as x). In reality, it should be noted that photobleaching would lead to a loss of fluorescence intensity, and as $x \rightarrow 1$, signal-to-noise ratio could be a limiting factor. For a population of dimers, progressive photobleaching would lead to a gradual increase in anisotropy. For a pure population of dimers, the anisotropy of the dimer is given by r_2 ($r_2 < r_1$). Since each monomer contains one fluorophore, three types of dimers would be generated (differing in the fluorescent state of the attached fluorophore) upon progressive photobleaching. These are: R*—R*, R*—R, and R—R where R* and R represent fluorescent and photobleached states of the fluorophore. Of these, R—R would be

nonfluorescent (dark) and therefore not contribute to the measured anisotropy. Assuming photobleaching to be random, the R*—R* population of dimers would be predominantly bleached for small values of *x*. With increase in the extent of photobleaching (*i.e*., with increasing *x*), the fraction of R*—R would increase. This species (R*—R) would be incapable of homo-FRET (due to the loss of a partner for homo-FRET). The anisotropy of R*—R would be essentially same as the monomeric anisotropy (r_1). In such a scenario, the resultant anisotropy of the population would change from r_2 (initial) to eventually to r_1, at the limit of fractional photobleaching $x \rightarrow 1$. This can be expressed binomially as:

$$r(2) = r_1 x + r_2(1-x)$$

where *r(2)* is the resultant anisotropy of the population as a function of *x*. Similarly, for a pure population of trimers, one obtains:

$$r(3) = r_1 x^2 + 2r_2 x(1-x) + r_3(1-x)^2$$

where *r(3)* corresponds to the resultant anisotropy of a trimeric population. Likewise, in case of tetramers, the resultant anisotropy is given by:

$$r(4) = r_1 x^3 + 3r_2 x^2(1-x) + 3r_3 x(1-x)^2 + r_4(1-x)^3$$

In general, for a homogeneous population of N-mer, the resultant anisotropy is given by:

$$r(N) = A_1 r_1 x^{(N-1)}(1-x)^0 + A_2 r_2 x^{(N-2)}(1-x)^1 + A_3 r_3 x^{(N-3)}(1-x)^2 + ... + A_N r_N x^0 (1-x)^{(N-1)}$$ Thes

e expressions are obtained by noting that for a population of N-mer, one has a polynomial of order (N-1) with the coefficients in the expansion (A_1, A_2, . . . A_N) derived from the $(N-1)^{th}$ row of the Pascal's triangle.

In a cellular milieu (particularly in a microheterogeneous media such as the biological membrane), a more realistic scenario would be the possible coexistence of various oligomeric forms in the same population. In order to address the change in fluorescence anisotropy upon photobleaching in such a population, we consider a Poisson distribution of monomers with the mean number corresponding to the order of oligomerization of the majority species in the population. For this, we consider a distribution of oligomers with oligomeric states 1 to N, each

with a corresponding mole fraction χ_N. The resultant anisotropy as a function of x can be then be described as:

$$r(N,\chi_N) = \sum_N N\chi_N r(N,x) \Big/ \sum_N N\chi_N$$

Interpretation of anisotropy data after photobleaching

As discussed above, the anisotropy enhancement after photobleaching can be interpreted in terms of oligomer size. For a monomeric population, the anisotropy as a function of fluorophore labeling (f) is invariant to photobleaching:

$$r^{monomer}(f) = r_1$$

For a dimeric population, the predicted anisotropy is given by:

$$r^{dimer}(f) = (1\text{-}f)r_1 + fr_2$$

where r_1 is the anisotropy of a singly-labeled dimer (R*—R; partially photobleached, no homo-FRET) and r_2 is the anisotropy of a doubly-labeled dimer (R*—R*). For a tetrameric population,

$$r^{tetramer}(f) = (1\text{-}f)^3 r_1 + 3f(1\text{-}f)^2 r_2 + 3f^2(1\text{-}f)\, r_3 + f^3 r_4$$

In the context of a mixed monomer-dimer-tetramer population, the total anisotropy as a function of labeling is given by the equation:

$$r^{total}(f) = a\, r(f)^{monomer} + b\, r^{dimer}(f) + (1\text{-}a\text{-}b)\, r^{tetramer}(f)$$

where a, b and (1-a-b) correspond to the monomer, dimer and tetramer fractions, respectively. In principle, fitting anisotropy enhancement after photobleaching to these equations should yield the required fractions. However, this analysis requires bleaching to completion, which is not possible in a realistic situation due to loss of intensity (as mentioned above) and possible cytotoxic effects. Instead, the initial anisotropy and the linearly extrapolated anisotropy can be used.

When all molecules are labeled, *i.e.*, $f = 1$,

$$r^{total} = a\, r^{monomer} + b\, r^{dimer} + (1\text{-}a\text{-}b)\, r^{tetramer}$$

The linearly extrapolated anisotropy, *i.e.*, apparent $f = 0$, is obtained by extrapolating the tangent to the function close to $f = 1$. The equations describing monomer, dimer and tetramer can be described as:

$$d(r(f)^{monomer})/df = 0;\ r(f = 0) = r_1$$

$$d(r(f)^{dimer})/df = r_2 - r_1;\ r(f = 0) = r_1$$

$$d(r(f)^{tetramer})/df = 3(r_4 - r_3);\ r(f = 0) = 3r_3 - 2r_4$$

It should be noted that the extrapolated anisotropies of monomers and dimers are equal to the monomeric anisotropy (only due to rotation), but the extrapolated anisotropy of tetramers (or other oligomers) is less than the monomeric anisotropy, provided $r_2 > r_4$. This results from the fact that anisotropy *vs*. labeling (photobleaching) curve for oligomers exhibits upward curvature. Using the linearly extrapolated anisotropy ($f = 0$),

$$r^{total}\ (f \rightarrow 0) = (a + b)\ r_1 + (1\text{-}a\text{-}b)(\ 3r_3 - 2r_4)$$

It follows that the fraction of oligomeric (in this example tetrameric) forms can be determined from the extrapolated anisotropy after photobleaching using the above equation. It is apparent from this equation that *the difference between the monomeric anisotropy and the extrapolated anisotropy is directly proportional to the fraction of oligomers*. This approach is particularly useful when comparing a series of measurements where a qualitative indication of relative amounts of oligomers is needed. For example, Bader et al. (2) estimated values for the relevant anisotropies for eGFP-tagged monomers, dimers and oligomers, to be: $r^{monomer} = 0.38$, $r^{dimer} = 0.31$, $r^{oligomer} = 0.276$.

Reference

1. Yeow EKL, Clayton AHA (2007) Enumeration of oligomerization states of membrane proteins in living cells by homo-FRET spectroscopy and microscopy: theory and application. *Biophys. J.* 92:3098-3104.

2. Bader AN, Hofman EG, Voortman J, en Henegouwen PM, Gerritsen HC (2009) Homo-FRET imaging enables quantification of protein cluster sizes with subcellular resolution. *Biophys. J.* 97:2613-2622.